A photo-responsive molecular wire composed of a porphyrin polymer and a fullerene derivative†

Hiroaki Ozawa,[a] Masahiro Kawao,[b] Shigeyasu Uno,[a] Kazuo Nakazato,[a] Hirofumi Tanaka[c] and Takuji Ogawa*[c]

Received 8th June 2009, Accepted 27th August 2009
First published as an Advance Article on the web 28th September 2009
DOI: 10.1039/b910638c

Dendron-protected porphyrin polymers ($M_n \sim 43\,000$ g mol^{-1}; $M_w \sim 111\,000$ g mol^{-1}) were deposited using the Langmuir–Blodgett method on glass surfaces modified with *N*-phenyl-3-aminopropyltriethoxysilane. These deposited films were soaked in a solution of a fullerene derivative bearing a pyridinyl moiety. Topographical images of the surface obtained by atomic force microscopy showed that the height of the porphyrin polymers was 3.1 ± 0.5 nm as deposited, and clearly increased to 3.9 ± 0.3 nm upon soaking. The increase in height (about 0.8 nm) corresponded to the diameter of the fullerene, indicating that the pyridinyl moieties of the fullerene molecules bound to the zinc atoms of the porphyrin units. Porphyrin polymers having thiol groups at both ends bridging nano-gapped gold electrodes were fabricated on silicon chips. The chips were soaked in the fullerene derivative solution to make devices containing porphyrin polymers whose central zinc atoms were coordinated by the fullerene derivative. The current–voltage (*I–V*) characteristics of these devices were measured, and higher conductivity was observed during photoirradiation only when the devices contained both the porphyrin polymer and the fullerene derivative; no photo-response was observed when either component was absent.

1. Introduction

Molecular electronics is a fascinating area of fundamental research with the potential for many applications.[1–6] Molecular wires play a key role in this research area. However, most organic molecules are not effective conductors because of their large energy gaps and ineffective carrier transport properties. Our strategy is to make them conductive by adding functional structures to "dope" such molecular wires. For example, porphyrin oligomers or polymers are typically neutral organic molecular wires[7–11] and their conductivities on the molecular scale are relatively low.[12,13] However, if they are connected to electron acceptors and irradiated, they can possibly become more conductive because of photo-doping caused by electron transfer from the porphyrin wires to the acceptors. Fullerene derivatives are attractive candidates for the latter because of their strong electron accepting properties[14,15] and low reorganization energy.[16] Due to this low reorganization energy and also the appropriate energy difference, photoinduced charge-separated states of porphyrin/fullerene assemblies have long lifetimes, and high quantum yields.[17–25] On account of these properties, porphyrin wires decorated with fullerene derivatives may work as efficient photo-switchable molecular wires, with higher conductivity during irradiation than in the dark (Fig. 1).

Fullerene–porphyrin dyads linked by covalent or non-covalent bonds have also been studied extensively as important components of solar energy conversion systems[16–20] and in molecular devices.[21,22] Most of these studies were performed in solution or on thin films in the solid state. We are interested in the electrical and optical properties of individual (or a small number of) assemblies on solid surfaces, with the aim of developing molecular-scale nano-devices.[23,24]

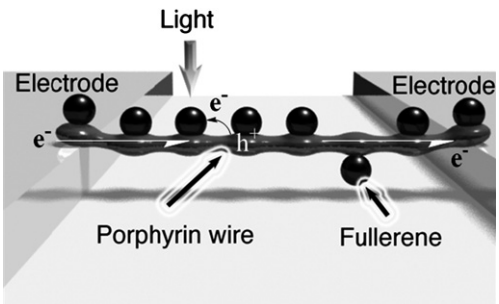

Fig. 1 Conceptual Figure of a photo-responsive molecular wire composed of porphyrin polymer and fullerenes (C_{60}). Photoexcitation of porphyrin polymer/fullerene composite transferred electrons from the porphyrin to the fullerene, forming holes in the former, through which current passed at a higher efficiency than in the ground state.

[a]*Department of Electrical Engineering and Computer Science, Graduate School of Engineering, Nagoya University, Furo-cho, Chikusa-ku, Nagoya, 464-8603, Japan. E-mail: nakazato@ nuee.nagoya-u.ac.jp; Fax: +81 (0)52 789 3139; Tel: +81 (0)52 789 3307*
[b]*Research Center for Molecular Nanoscience, Institute for Molecular Science, National Institutes of Natural Sciences, 5-1 Higashiyama, Myodaiji-cho, Okazaki Aichi, 444-8787, Japan. E-mail: bosabosa@ims.ac.jp; Fax: +81 (0)564 59 5510; Tel: +81 (0)564 59 5534*
[c]*Department of Chemistry Graduate School of Science, Osaka University, 1-1 Machikaneyama, Toyonaka, Osaka, 560-0043, Japan. E-mail: ogawa@chem.sci.osaka-u.ac.jp; Fax: +81 (0)6 6850 5395; Tel: +81 (0)6 6850 5392*

† Electronic supplementary information (ESI) available: Analytical GPC data of dendron protected porphyrin, thiol group capped porphyrin polymers; UV-Vis spectra of the sum of the spectra of **1** and **2**, and *I–V* measurement of other devices. See DOI: 10.1039/b910638c

Here we report the preparation of π-conjugated porphyrin wires whose central Zn atoms were coordinated by pyridinyl-substituted fullerene **2** (Chart 1). The structure and electronic properties of the wires were studied by atomic force microscopy (AFM) and spectroscopic methods. Furthermore, their electrical properties were studied by fabricating nano-devices using gold electrodes with *ca.* 10 nm gaps made by a molecular self-assembly method.[26–28]

2. Experimental

All reagents and solvents were of analytical grade and used without further purification. Compounds **1**, **2**, **3**, and, **4** were synthesized according to the literature.[29–31] Silane-modified glass substrates were prepared according to the literature.[29] UV-Vis absorption spectra were recorded with a Shimadzu UV-3150 double-beam spectrophotometer and fluorescence spectra with a JASCO FP-6600 spectrometer. Analytical gel permeation chromatography (GPC) data were recorded on a JASCO MD-2015 Plus with Shodex GPC KF-804L and 805L columns, using THF as the mobile phase at a flow rate of 1 ml min^{-1}. NMR spectra were recorded on a JEOL JNM-LA400 spectrometer relative to the TMS internal standard ($\delta = 0.00$). Porphyrin polymers were deposited on substrates using a Nihon Laser NL-LB 400 Langmuir–Blodgett film system. Atomic force microscopy (AFM) was performed with a JEOL JSPM-4210 instrument. All images were collected in tapping mode in air with a silicon cantilever (Mikromasch, silicon cantilevers NSC35/AIBS/50). A Hitachi S-4300 scanning electron microscope (SEM) was used in this work. The *I–V* curves were collected by an Advantest R6245 2 Channels voltage–current source monitor interfaced to a microcomputer through a GPIB-SCSI board using the NI-488.2 protocol. The data were acquired with a homemade procedure and IgorPro 4.0 (Wavemetrics) software. The samples were mounted on an anti-vibration table in a temperature-controlled cryogenic chamber (±0.005 K). All measurements were carried out in high vacuum ($P < 2.0 \times 10^{-4}$ Pa) achieved by means of a turbo pump, and the samples were cooled using liquid helium (10 to 300 K). Triaxial cables were used to connect the molecular devices and the *I–V* monitor in order to minimize external noise.

The assembly of fullerene derivative **2** linked to porphyrin polymer **1** was deposited on modified glass surfaces as follows: dendron-protected porphyrin polymer **1** ($M_n \sim 43\,000$ g mol^{-1}; $M_w \sim 111\,000$ g mol^{-1}) was collected by analytical GPC (Fig. 1S in the ESI†), dissolved in DMF–chloroform (1 : 1), and diluted with the same solvent to adjust the absorbance to about 0.1 at 461 nm. Droplets of this solution were spread on the water surface of the LB trough. After being left undisturbed for 10 min, the barrier was moved at 3 mm min^{-1} to compress the surface film, while the dipper with the substrate (glass surface modified with *N*-phenyl-3-aminopropyltriethoxysilane)[29] was moved vertically upward at 3 mm min^{-1}, keeping the interface pressure at 1 mN m^{-1}. The substrates thus prepared were dried in air and observed by AFM, then soaked in a toluene solution of the modified fullerene **2** (0.1 mg mL^{-1}) for 1 min, followed by washing with toluene and drying with nitrogen gas, and were observed by AFM again.

Gold electrodes with *ca.* 10 nm gaps were prepared using a molecular ruler method.[26–28] The parent electrodes composed of Au (130 nm)/Ti (15 nm) were patterned by photolithography. Ten

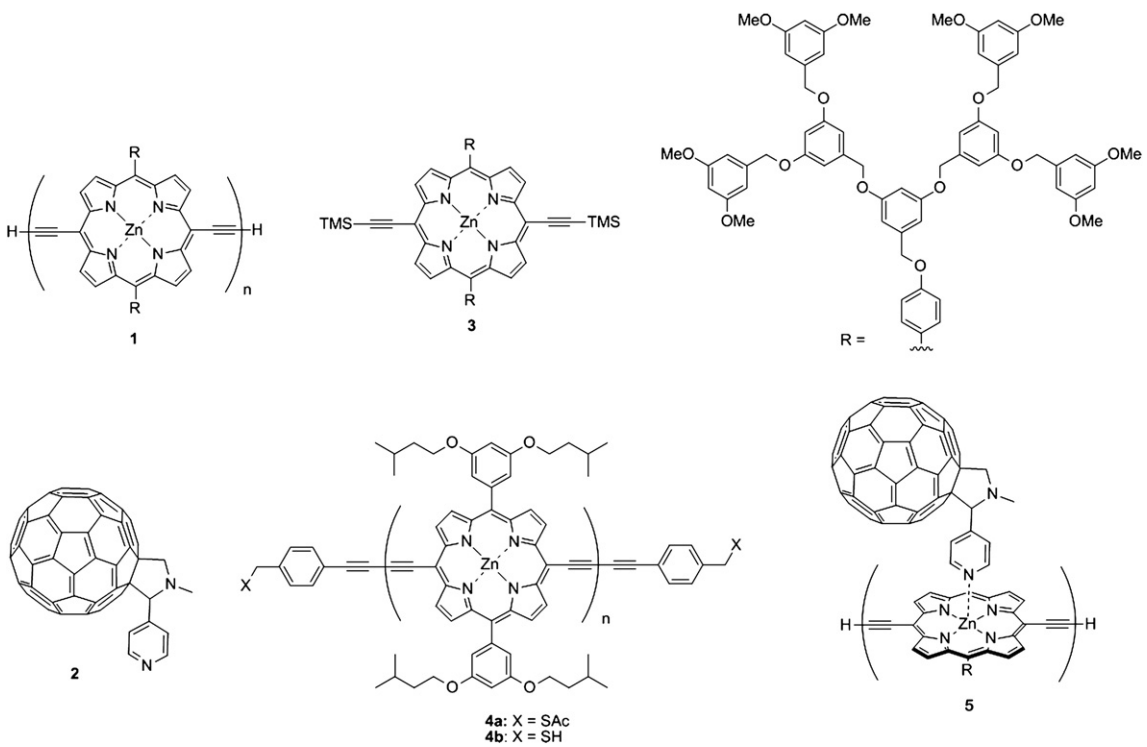

Chart 1 Structures of dendron-protected porphyrin polymer **1**; fullerene derivative **2**; monomer **3**; thiol-capped porphyrin polymers **4a** and **4b**; and assembly polymer with fullerene derivatives **5**.

layers of SAM films were formed on the parent electrodes as a size-controlled resist. The daughter electrodes Au (50 nm)/Ti (15 nm) were then evaporated on these using photolithography. The SAM resists were removed with N-321 remover to form a nano-gap between the parent and the daughter electrodes. The gap size estimated from SEM images (Fig. 5) was approximately 10 nm, which corresponded well to the thickness of the SAM film.

Porphyrin polymers **4b** capped with thiol groups were dissolved in THF (0.1 mg ml^{-1}). Aqueous NH_3 was added to the solution, in which the above-mentioned electrodes were soaked for one day. The electrodes were washed with THF and methanol and dried using nitrogen gas. A solution of fullerene derivative **2** (0.1 mg ml^{-1} in toluene) was added dropwise onto the electrodes, which were then washed with toluene and methanol and dried using nitrogen gas.

3. Results and discussion

To improve imaging by scanning probe microscopy (SPM), the diameter of the molecular wire was increased by introducing the dendron moieties shown in Chart 1. The dendron-protected porphyrin monomer **3**, polymer **1**, and fullerene (C_{60}) derivative **2** were prepared by previously reported methods.[29,30] Dendron-protected porphyrin polymers ($M_n \sim 43\,000$ g mol^{-1}; $M_w \sim 111\,000$ g mol^{-1}; the molecular weight of each monomer unit was 2473 g mol^{-1}; see Fig. 1S†for the GPC chart) were used in these experiments after fractionation by gel permeation chromatography (GPC).

Porphyrin polymers capped at both ends by thiol groups (**4**), which were capable of bridging the gold electrodes with nano-scale gaps, were prepared by the reported method.[31] The thiol-capped porphyrin polymers **4** were fractionated by GPC and a fraction with $M_n \sim 6460$ g mol^{-1} and $M_w \sim 17200$ g mol^{-1} (molecular weight of the monomer unit = 853 g mol^{-1}; see Fig. 2S† for the GPC chart) was used.

Composites containing porphyrin polymer **1** and fullerene derivative **2** were prepared by below two methods. Method 1. A solution of porphyrin polymer 1 (absorbance ~ 0.3 at 463 nm in $CHCl_3$) was mixed with a solution of the fullerene derivative **2** (0.1 mg ml^{-1} in $CHCl_3$). The mixed solution was used for further spectroscopic analyses. Method 2. Porphyrin polymers were dispersed on substrate surfaces using the Langmuir–Blodgett method, resulting in network structures, as observed by AFM. These substrates were immersed in a solution of the fullerene derivative **2** for 2 min, dried, and finally rinsed with toluene.

In order to ascertain that the fullerene derivative **2** could coordinate to the dendron-protected Zn-porphyrin in solution, the ^{1}H NMR spectrum of a mixture of **2** and the porphyrin monomer **3** in $CDCl_3$ was analyzed. The protons at the β-position of the porphyrin ring of **3** exhibited peaks at 9.63 and 8.87 ppm (Fig. 2(a)), which shifted to 9.57 and 8.81 ppm, respectively, upon addition of **2** (Fig. 2(b)). Furthermore, the peaks of the dendron moieties also shifted (Fig. 3S, see the ESI†). None of the foregoing peaks shifted at all when unmodified fullerene was added (Fig. 2(c)).

UV-Vis absorption spectra in $CHCl_3$ of the porphyrin polymer **1**, fullerene derivative **2** and the assembly (**1** + **2**) are shown in Fig. 3(a). In comparison with **1**, the Soret and Q band bands of assembly were red-shifted by approximately 1 nm, respectively.

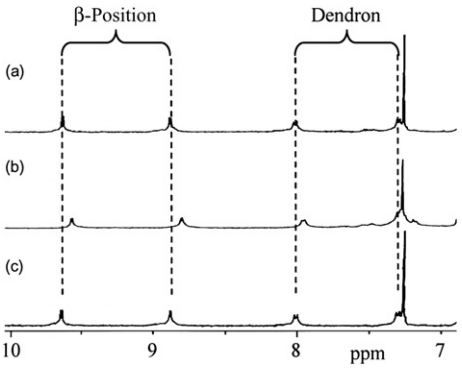

Fig. 2 ^{1}H NMR spectra of (a) porphyrin monomer **3**, (b) a mixture of **3** and fullerene ligand **2**, and (c) a mixture of **1** and unmodified fullerene, all in $CDCl_3$.

The results reveal the formation of assembly *via* coordination bonds. The spectrum of the assembly could be superimposed on the summed spectra of **1** and **2** (Fig. 4S, see the ESI†), indicating minimal electronic interaction between the two components, consistent with previous reports.[29,32] Fluorescence spectra of the assemblies and of the porphyrin polymer are shown in Fig. 3(b). The emission of **1** (in $CHCl_3$, centered at 814 nm, excitation at 465 nm) was quenched in the assembly (**1** + **2**). The quenching was most likely caused by electron transfer from porphyrin polymer **1** to fullerene ligand **2**, as has been observed for other porphyrin-fullerene dyads.[32,33]

Fig. 4 shows AFM images of the porphyrin polymer on a modified glass surface before (Fig. 4(a)) and after (Fig. 4(b)) treatment with fullerene derivative **2**. The average height of the

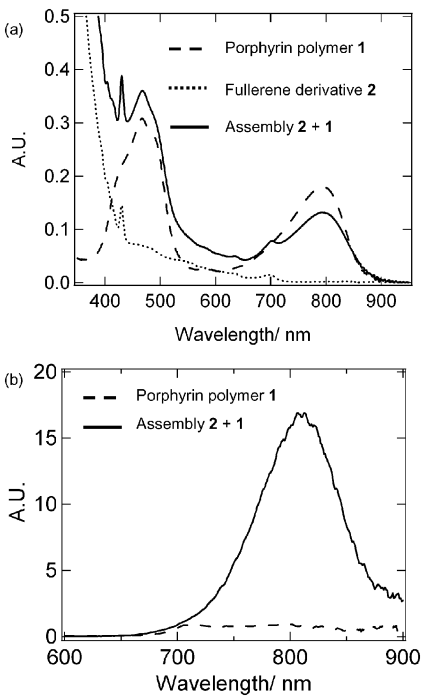

Fig. 3 (a) UV-Vis absorption spectra in $CHCl_3$ of porphyrin polymers **1**, fullerene ligand **2**, and a mixture of **1** and **2**. (b) Fluorescence spectra of **1** and a mixture of **1** and **2** in $CHCl_3$ (excitation wavelength 465 nm).

assembly (**1 + 2**) (3.9 ± 0.3 nm, Fig. 4(d)) was *ca.* 0.8 nm higher than that of the porphyrin polymer **1** (3.1 ± 0.5 nm, Fig. 4(c)); the difference was almost identical to the size of the fullerene ligand, strongly indicating that the fullerene derivative **2** was connected to the porphyrin polymer molecules. AFM images of porphyrin polymers treated with fullerene C_{60} instead of **2** showed no change in average height, confirming that fullerene C_{60} without a pyridinyl moiety did not connect to the porphyrin polymer.

These experiments confirmed that fullerene derivative **2** could coordinate to the zinc atom of the porphyrin units in the polymer, and that the excited state of the porphyrin could be quenched efficiently, probably by electron transfer to the fullerene moiety (Fig. 1). We next fabricated photo-responsive electronic devices using this molecular system. In order to bridge the nanoscale gap between the gold electrodes, a porphyrin polymer having thiol (–SH) groups at both ends (**4b**) was used. The average length of the polymer was estimated at *ca.* 17 nm based on GPC analysis (Fig. 2S†). Devices were fabricated with a well-defined gap of 10 nm between electrodes, using molecular ruler methods.[26–28] The SEM images of these electrodes with their nanoscale gaps are shown in Fig. 5. The length of porphyrin polymer molecules **4b** was estimated to be sufficient to bridge the gap between these electrodes. Devices made using this molecular assembly and these electrodes were prepared as follows: aqueous NH_3 was added to a THF solution of the porphyrin polymers with acetyl protected thiols at both ends (**4a**) to remove the acetyl groups, and the electrodes on silicon chips were soaked in this solution for 1 day. The electrodes were washed with THF and methanol, dried using nitrogen gas, and finally soaked in a solution of fullerene derivative **2**. These electrodes were then washed with toluene and methanol, and dried with nitrogen gas.

The *I–V* curves of the devices were measured at room temperature under vacuum (~2×10^{-4} Pa). The measurements started at a bias of −5 V, which increased to +5 V and then returned to −5 V. Without the porphyrin polymers, the electrodes were completely non-conductive in this bias range as in the typical example shown in Fig. 6(a) (dotted line). After bridging

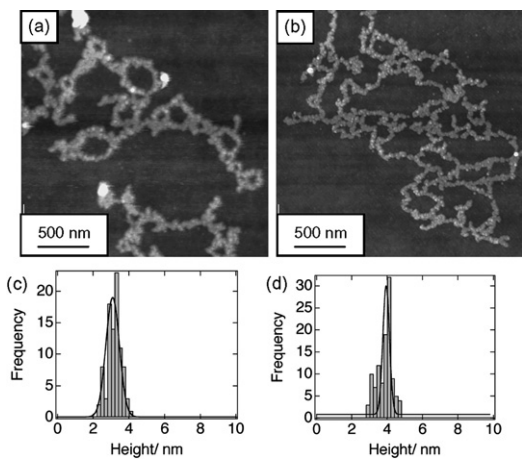

Fig. 4 AFM images of (a) porphyrin polymers **1** and (b) assembly (**1 + 2**) on modified glass surfaces. Histograms of (c) **1** with height 3.1 ± 0.5 nm and of (d) assembly (**1 + 2**) with height (3.9 ± 0.3 nm).

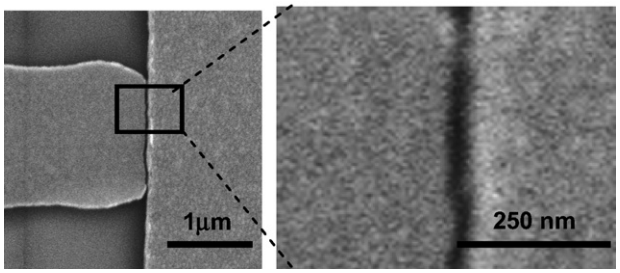

Fig. 5 Left: SEM image of electrodes with a nanoscale gap fabricated by a molecular ruler method. Right: magnified image.

with porphyrin polymers, the conductivity clearly increased at high bias (Fig. 6(a), broken line). Upon coordination with fullerene derivative **2**, the conductivity increased dramatically (Fig. 6(a), solid line).

When these devices were irradiated with a metal halide lamp through a quartz fiberglass waveguide, a sharp increase in conductivity was observed, as shown in Fig. 6(b) and 6(c). Almost no photo-response was observed without the fullerene derivative. The possibility of thermal effects caused by the irradiation could be excluded because the devices without the fullerene derivative exhibited a minimal photo-response (Fig. 5S, ESI†). If there had been a thermal effect the devices with only the porphyrin array should have shown a similar photo-response. The reproducibility was qualitatively confirmed with six devices prepared similarly (Fig. 6S, ESI†). As control experiments, devices containing only the fullerene derivative **2** were analyzed—no conductivity was observed in these devices.

In order to understand the mechanism of conduction in these devices, their temperature dependence was studied in the range from 10 to 300 K. The *I–V* curves of a typical device are shown in Fig. 7(a), exhibiting a sigmoid shape over this temperature range. The Arrhenius plots of the current are shown in Fig. 7(b) at various voltages.

The Arrhenius plots were composed of more than two linear regions at any voltage, which probably meant that more than two conduction mechanisms were active. At low temperature (10–70 K), the currents were temperature-independent, and above 70 K ($1/T \sim 0.14$) thermal excitation dominated the conduction behavior (Fig. 7(b)). Several models have been proposed to explain the *I–V–T* dependence of such devices: At low temperatures (10–70 K), it was reasonable to think that electron transfer was governed by tunneling processes, considering the temperature independence of these results. These tunneling processes were further divided into Fowler–Nordheim tunneling and direct tunneling.

Temperature independent mechanisms:

$$\text{Fowler–Nordheim tunneling} \quad I \sim V^2 \exp\left(-\frac{4d\sqrt{2m}}{3\text{q}\hbar V}(q\phi)^{1.5}\right)$$

$$\text{Direct tunneling} \quad I \sim V \exp\left(-\frac{4\pi d}{h}\sqrt{2m\phi}\right)$$

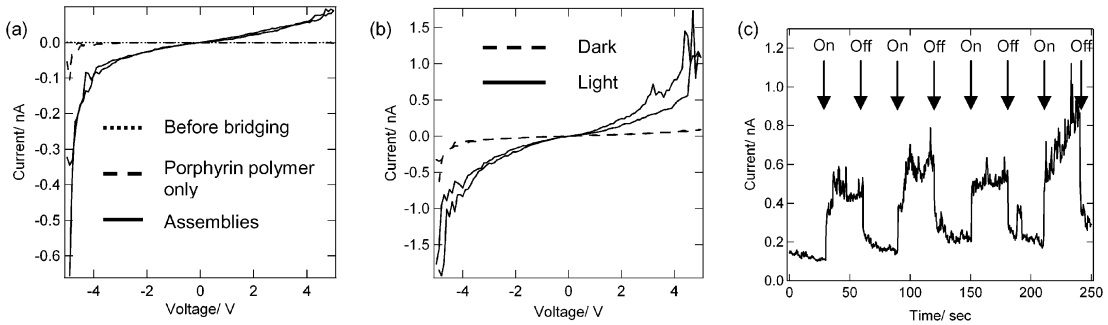

Fig. 6 (a) *I–V* curves measured at room temperature for the gapped electrode as-cleaned (dotted lines), after bridging with porphyrin polymer **4** (broken lines), and for the device treated with fullerene derivative **2** (solid lines). (b) Photo-response *I–V* curves of the device. *I–V* curves under irradiation (solid lines) and in the dark (broken lines). (c) Photo-response behavior of the device fabricated with porphyrin polymer **4** and fullerene derivative **2**.

Temperature dependent mechanisms:

$$\text{Hopping conduction} \quad I \sim V\exp\left(-\frac{\Delta E}{kT}\right)$$

$$\text{Thermionic emission} \quad I \sim T^2\exp\left(-q\frac{\phi-\sqrt{\frac{qV}{4\pi\varepsilon d}}}{kT}\right)$$

These two tunneling mechanisms could be distinguished from the voltage dependence of the *I–V* characteristics of the device.[34,35] In Fowler–Nordheim tunneling, $\ln(I/V^2)$ is linear with respect to $1/V$, while in direct tunneling I is linearly dependent on V. As shown in Fig. 7(c), in the high bias range ($1/V < 0.4$, $V > 2.5$), $\ln(I/V^2)$ was almost linearly dependent on $1/V$, but not in the lower bias range ($1/V > 0.4$, $V < 2.5$). The interpretation of these results was that Fowler–Nordheim tunneling was dominant at higher bias, and direct tunneling at lower bias.

The results from the higher temperature region (70–300 K) were explained by thermionic emission,[34] because with a hopping mechanism I would vary linearly with V.[34] Fig. 7(d) shows the $\ln(I/T^2)$ *vs.* $1/T$ plots, which were fairly linear.

The *I–V* curves and the photo-response of a typical device measured at 100, 200, and 300 K are shown in Fig. 8. The device was fabricated on a silicon chip (5 × 5 × 0.1 mm) and placed directly on the heat sink of a measuring probe, whose temperature was controlled by a cryostat to within 0.5 K. Since the heat capacity of the chip was negligibly small, the surface temperature did not increase substantially during irradiation.

Two important findings from the results shown in Fig. 8 were that the ratio I_{light}/I_{dark} increased at high voltage and low temperature. As discussed in a previous section, a tunneling mechanism

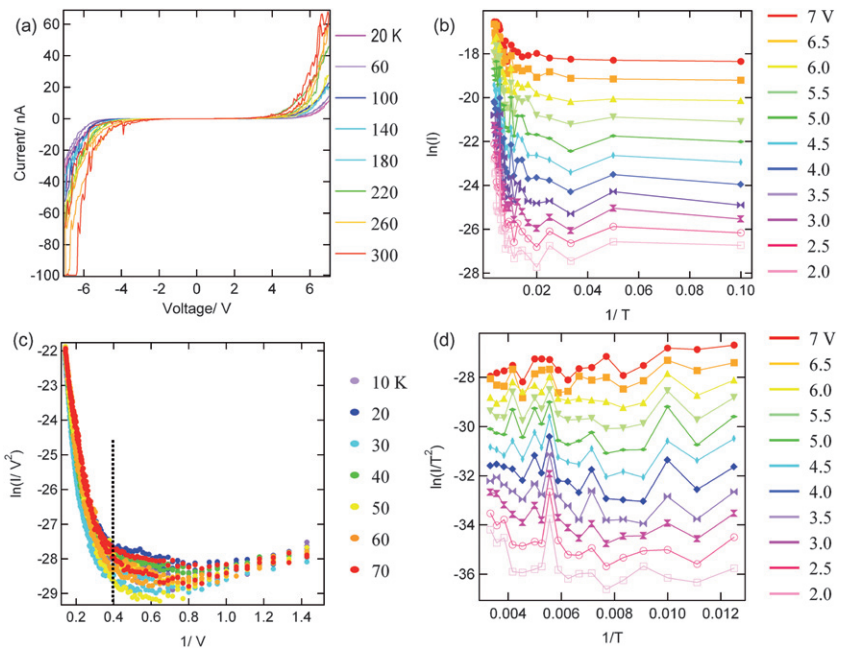

Fig. 7 (a) Temperature dependent *I–V* characteristics of a device. (b) Arrhenius plots for the range 2.0–7.0 V (interval 0.5 V). (c) A series of plots of $\ln(I/V^2)$ *vs.* $1/V$ at temperatures from 10 K to 70 K, in 10 K increments. (d) A series of plots of $\ln(I/T^2)$ *vs.* $1/T$ at biases from 2.0–7.0 V.

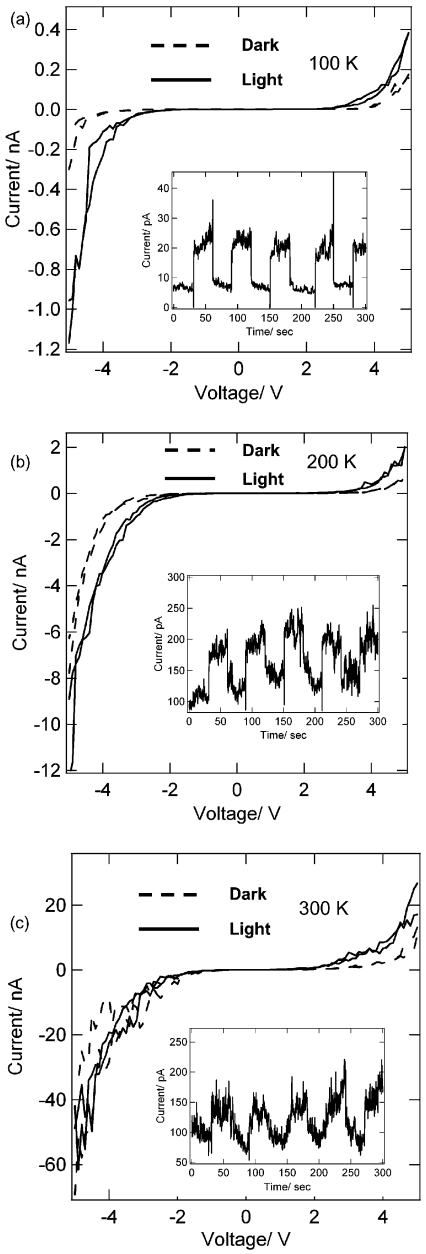

Fig. 8 Reversible photo-response *I–V* and *I–T* curves of the device. A time-current scan mode with 0.3 s intervals was used for 300 s to record the process of the photo-response, and the light source was switched periodically. (a) *I–V* curves under irradiation (solid lines) and in the dark (broken lines) in the range −5 to +5 V at 100 K. The inset is the *I–T* curve when the light was turned on and off periodically at 100 K. (b) and (c) *I–V* curves under irradiation (solid lines) and in the dark (broken lines) in the range −5 to +5 V at 200 and 300 K, respectively. The insets show *I–T* curves when the light was turned on and off periodically at 200 and 300 K, respectively.

predominated at low temperature, with thermionic emission commencing as the temperature increased. Thus, these results indicated that light irradiation affected the tunneling more than it did the thermionic emission. In addition, this effect was larger for the Fowler–Nordheim tunneling operational at high voltage.

If the photo-response of the devices had been due to the usual photo-generated carrier mechanism, it should have displayed temperature independence, because charge carriers would have been generated by thermionic emission as well as by photo-irradiation. However, this was not the case for these devices. Photoexcitation of this [porphyrin array/fullerene] system probably generated charge-separated excited states such as [porphyrin array$^{(+\cdot)}$/fullerene$^{(-\cdot)}$], with a smaller tunneling barrier in the porphyrin array$^{(+\cdot)}$ than in the neutral porphyrin array, leading to increased conductivity. Although further detailed mechanistic studies are required to identify the precise mechanism of conduction, such photo-gated switches are clearly fascinating and potentially useful molecular devices.

Conclusions

In conclusion, one-dimensional assemblies could be fabricated by binding fullerene ligand **2** to conjugated porphyrin polymers **1**. The assembled structures were examined by AFM.

The electrical devices prepared from the assemblies showed photo-responsive conduction. Both **1** and **2** were indispensable for the photo-response. Temperature dependent *I–V* measurements showed multiple conduction mechanisms: at low temperatures, tunneling took place, while thermionic emission was responsible for conduction at high temperatures. It was likely that a photo-doped state was responsible for reducing the tunneling resistance of the composite of **1** and **2**.

Acknowledgements

This work was supported by Grants-in-Aid for Scientific Research (No. 19310079 and 20111012) from the Ministry of Culture, Education, Science, Sports, and Technology of Japan.

Notes and references

1 J. M. Tour, *Chem. Rev.*, 1996, **96**, 537.
2 M. A. Reed, C. Zhou, M. R. Deshpande, C. J. Muller, T. P. Burgin, L. Jones and J. M. Tour, *Ann. N. Y. Acad. Sci.*, 1998, **852**, 133.
3 M. A. Reed, *Proc. IEEE*, 1999, **87**, 652.
4 J. Chen, W. Wang, J. Klemic, M. A. Reed, B. W. Axelrod, D. M. Kaschak, A. M. Rawlett, D. W. Price, S. M. Dirk, J. M. Tour, D. S. Grubisha and D. W. Bennett, *Ann. N. Y. Acad. Sci.*, 2002, **960**, 69.
5 J. M. Tour, W. L. Van Zandt, C. P. Husband, S. M. Husband, L. S. Wilson, P. D. Franzon and D. P. Nackashi, *IEEE Trans. Nanotechnol.*, 2002, **1**, 100.
6 T. H. Lee, W. Y. Wang and M. A. Reed, *Ann. N.Y. Acad. Sci.*, 2003, **1006**, 21.
7 A. O. Orlov, I. Amlani, G. H. Bernstein, C. S. Lent and G. L. Snider, *Science*, 1997, **277**, 928.
8 A. Osuka and H. Shimidzu, *Angew. Chem., Int. Ed. Engl.*, 1997, **36**, 135.
9 T. Ogawa, Y. Nishimoto, N. Yoshida, N. Ono and A. Osuka, *Chem. Commun.*, 1998, 337.
10 T. Ogawa, Y. Nishimoto, N. Yoshida, N. Ono and A. Osuka, *Angew. Chem., Int. Ed.*, 1999, **38**, 176.
11 K. Ogawa and Y. Kobuke, *Angew. Chem., Int. Ed.*, 2000, **39**, 4070.
12 H. Tanaka, T. Yajima, M. Kawao and T. Ogawa, *J. Nanosci. Nanotechnol.*, 2006, **6**, 1644.
13 H. Tanaka, T. Yajima, T. Matsumoto, Y. Otsuka and T. Ogawa, *Adv. Mater.*, 2006, **18**, 1411.
14 T. Drovetskaya, C. A. Reed and P. Boyd, *Tetrahedron Lett.*, 1995, **36**, 7971.
15 H. Imahori, K. Hagiwara, T. Akiyama, S. Taniguchi, T. Okada and Y. Sakata, *Chem. Lett.*, 1995, 265.
16 H. Imahori, K. Hagiwara, T. Akiyama, M. Aoki, S. Taniguchi, T. Okada, M. Shirakawa and Y. Sakata, *Chem. Phys. Lett.*, 1996, **263**, 545.

17 H. Imahori, K. Yamada, M. Hasegawa, S. Taniguchi, T. Okada and Y. Sakata, *Angew. Chem., Int. Ed. Engl.*, 1997, **36**, 2626.
18 K. Tamaki, H. Imahori, Y. Nishimura, I. Yamazaki, A. Shimomura, T. Okada and Y. Sakata, *Chem. Lett.*, 1999, 227.
19 P. A. Troshin, R. Koeppe, A. S. Peregudov, S. M. Peregudova, M. Egginger, R. N. Lyubovskaya and N. S. Sariciftci, *Chem. Mater.*, 2007, **19**, 5363.
20 A. Kira, T. Umeyama, Y. Matano, K. Yoshida, S. Isoda, J. K. Park, D. Kim and H. Imahori, *J. Am. Chem. Soc.*, 2009, **131**, 3198.
21 M. E. El-Khouly, R. Anandakathir, O. Ito and L. Y. Chiang, *J. Phys. Chem. A*, 2007, **111**, 6938.
22 N. K. Subbaiyan, I. Obraztsov, C. A. Wijesinghe, K. Tran, W. Kutner and F. D'Souza, *J. Phys. Chem. C*, 2009, **113**, 8982.
23 S. Gadde, D. M. S. Islam, C. A. Wijesinghe, N. K. Subbaiyan, M. E. Zandler, Y. Araki, O. Ito and F. D'Souza, *J. Phys. Chem. C*, 2007, **111**, 12500.
24 A. Kotiaho, R. M. Lahtinen, N. V. Tkachenko, A. Efirnov, A. Kira, H. Imahori and H. Lemmetyinen, *Langmuir*, 2007, **23**, 13117.
25 D. Wrobel, A. Graja, H. Manikowski and K. Lewandowska, *Chem. Phys.*, 2007, **336**, 165.
26 M. E. Anderson, M. Mihok, H. Tanaka, L. P. Tan, M. W. Horn, G. S. McCarty and P. S. Weiss, *Adv. Mater.*, 2006, **18**, 1020.
27 H. Tanaka, M. E. Anderson, M. W. Horn and P. S. Weiss, *Jpn. J. Appl. Phys.*, 2004, **43**, L950.
28 R. Negishi, T. Hasegawa, K. Terabe, M. Aono, H. Tanaka, T. Ogawa and H. Ozawa, *Appl. Phys. Lett.*, 2007, **90**, 223112.
29 H. Ozawa, M. Kawao, H. Tanaka and T. Ogawa, *Langmuir*, 2007, **23**, 6365.
30 F. D'Souza, G. R. Deviprasad, M. E. Zandler, V. T. Hoang, A. Klykov, M. VanStipdonk, A. Perera, M. E. El-Khouly, M. Fujitsuka and O. Ito, *J. Phys. Chem. A*, 2002, **106**, 3243.
31 H. Ozawa, M. Kawao, H. Tanaka and T. Ogawa, *Tetrahedron*, 2006, **62**, 4749.
32 S. R. Wilson, S. MacMahon, F. T. Tat, P. D. Jarowski and D. I. Schuster, *Chem. Commun.*, 2003, 226.
33 P. Cheng, S. R. Wilson and D. I. Schuster, *Chem. Commun.*, 1999, 89.
34 M. A. Reed, T. Lee, *Molecular Nanoelectronics*, American Scientific Publishers: Los Angeles, California, 2003, pp. 39–114.
35 W. P. Hu, H. Nakashima, K. Furukawa, Y. Kashimura, K. Ajito, C. Han and K. Torimitsu, *Phys. Rev. B: Condens. Matter Mater. Phys.*, 2004, **69**, 165207.